Supplementary Information for

Mechanism of Selective Benzene Hydroxylation Catalyzed by Iron-Containing Zeolites

Benjamin E. R. Snyder[a,†], Max L. Bols[b], Hannah M. Rhoda[a], Pieter Vanelderen[a,b], Lars H. Böttger[a], Augustin Braun[a], James J. Yan[a], Ryan G. Hadt[a,‡], Jeffrey T. Babicz, Jr.[a], Michael Y. Hu[c], Jiyong Zhao[c], E. Ercan Alp[c], Britt Hedman[d], Keith O. Hodgson[a,d], Robert A. Schoonheydt[b,*], Bert F. Sels[b,*], and Edward I. Solomon[a,d,*]

[a]Department of Chemistry, Stanford University, Stanford, California 94305, United States
[b]Department of Microbial and Molecular Systems, Centre for Surface Chemistry and Catalysis, KU Leuven – University of Leuven, Celestijnenlaan 200F, B-3001 Leuven, Belgium.
[c]Advanced Photon Source, Argonne National Laboratory, Argonne, IL 60439
[d]Stanford Synchrotron Radiation Lightsource, SLAC National Accelerator Laboratory, Stanford University, Menlo Park, CA 94025
[†]Current address: Department of Chemistry, University of California, Berkeley, California 94720, United States.
[‡]Current address: Division of Chemistry and Chemical Engineering, California Institute of Technology, Pasadena, California 91125, United States.

Robert A. Schoonheydt: robert.schoonheydt@kuleuven.be
Bert F. Sels: bert.sels@kuleuven.be
Edward I. Solomon: solomone@stanford.edu

This PDF file includes:

SI Methods

Preparation of Fe-zeolites. Samples of Fe-BEA (Si/Al=12.5) and Fe-ZSM-5 (Si/Al=15) were prepared from the corresponding acid zeolites by diffusion impregnation of $Fe(acac)_3$ (acac = acetylacetonate) in toluene solution (2.5 mM; 25 ml/g zeolite), resulting in Fe loadings of ~0.3 wt%. ^{57}Fe-enriched Fe-zeolites were synthesized similarly using 100% $^{57}Fe(acac)_3$. After Fe impregnation, all samples were calcined in air at 550 °C to remove organic material. This preparation method maximizes Fe homogeneity and limits the formation of oxide/hydroxide species.[1] Samples were then subjected to a high-temperature treatment at 900 °C in He (20 cm^3/min) for 2 hours, followed by a reductive treatment in H_2 at 700 °C for 1 hour (20 cm^3/min). All subsequent manipulations were carried out under an inert atmosphere (either nitrogen or helium). All sample treatment procedures and reactions were carried out in a quartz reactor containing a 2.4 cm^3 bed of pelletized zeolite (250-500 μm), corresponding to 0.8 g of material. N_2O activation of reduced Fe(II)-BEA and Fe(II)-ZSM-5 was performed at 160 °C using a 5 vol% N_2O/He flow (20 cm^3/min). For Fe-ZSM-5, labeled α-^{18}O was prepared by treating a sample of N_2O-activated Fe-ZSM-5 in an atmosphere of pure $^{18}O_2$ at 100 °C for 30 hours. A typical sample of N_2O-activated Fe-BEA (0.3 wt% Fe, Si/Al = 12) contains ~ 40 μmol α-O per gram of catalyst (~80% of total Fe content). The C_6H_6 reaction was performed at room temperature using a flow He gas saturated with C_6H_6 vapor (20 cm^3/min).

Diffuse reflectance spectroscopy. DR-UV-vis spectra were recorded on a Varian Cary 5000 UV–VIS–NIR spectrophotometer at room temperature against a halon white reflectance standard. All treatments before the in situ UV-vis-NIR spectroscopic measurements were performed in a quartz U-tube/flow cell. The latter was equipped with a window for in situ UV-vis-NIR diffuse reflectance spectroscopy. After UV-vis measurements, the catalyst pellets were mounted in the quartz side arm of the U-tube, ensuring that the conditions for UV-vis-NIR and other spectroscopic measurements were identical.

Mössbauer spectroscopy. ^{57}Fe Mössbauer spectra were recorded with a See Co. W302 resonant gamma ray spectrometer in horizontal geometry with zero external field using a 1.85 GBq source (Be window, Rh matrix). Data were collected from samples enriched with 100% ^{57}Fe. Spectra were recorded at 6K, and isomer shifts are given relative to α-Fe_2O_3 foil at room temperature. Spectra were collected with 1,024 points and summed up to 256 points before analyzing, and then fit with Lorentzian doublets using the Vinda software package for Microsoft Excel.[2]

MCD and VTVH-MCD spectroscopy. Cells for MCD spectroscopy were prepared under an inert nitrogen atmosphere. Mull samples with suitable transparency were prepared using dried and degassed perfluoro-2-methylpentane as the mulling agent. Mulls were frozen using liquid nitrogen immediately after preparation. MCD data were collected using a Jasco J730 spectropolarimeter with a liquid nitrogen cooled InSb

detector coupled to an Oxford Instruments SM4000-7T superconducting magnet. MCD spectra were background corrected for baseline effects using data collected at 0 T. VTVH-MCD data were collected using a calibrated Cernox temperature sensor (Lakeshore Cryotronics, calibrated to 1.5–300 K with 0.001 K tolerance) inserted directly into the sample cell. Isotherms/isofields were normalized to the maximum observed intensity. Spin Hamiltonian parameters were extracted from VTVH-MCD isotherms using established procedures.[3]

XAS spectroscopy. XAS cells (2 mm x 10 mm capped-type Delrin cells wrapped with Kapton tape) were loaded under an inert N_2 atmosphere with zeolite powder suspended in perfluoro-2-methylpentane, and then frozen under liquid nitrogen. The samples were oriented at 45° to the incident X-ray beam and maintained at 10 K using an Oxford Instruments CF1208 continuous flow liquid helium cryostat. XAS data were collected at beamlines 7-3 and 9-3 at the SSRL under ring operating conditions of 500 mA over an energy range of 6,785–7,876 eV (k=14 $Å^{-1}$). Fluorescence data were collected at 90° to the incident beam using a solid-state 30- or 100-element Ge detector array with Soller slits and a six-wavelength Mn filter aligned between the detector and the sample to improve the Fe Kα fluorescence signal intensity relative to that of the scattered beam.[4] An internal calibration was utilized with the first inflection point of an Fe foil set to 7,111.2 eV.[5] During measurement, the data in the Fe K-edge, K pre-edge, and EXAFS regions were continuously monitored to ensure sample integrity by comparing each individual scan to ones taken previously. To minimize photodamage, different spots

were scanned along the samples and averaged, and only the first scan on each spot was included in the reported data.

Data reduction, background subtraction, and normalization were performed according to established methods[6–8] using the program PySpline[9] with the data normalized to a value of 1.0 at 7,130.0 eV. The spline function through the EXAFS region was chosen to minimize any residual low-frequency background but not reduce the EXAFS amplitude, as monitored by the Fourier transform intensity. Normalization of the EXAFS data was accomplished using a third-order postedge polynomial background fit over the full data range (k=14 Å^{-1}) and a three-segment (four-knot) spline.

EXAFS signals were calculated using FEFF (version 7.0), and the data were fit using the program OPT as part of EXAFSPAK.[10] In all fits the bond lengths (R) and bond variances (σ^2) were allowed to vary. The threshold energy (k=0, E_0) was also allowed to vary but was constrained as a common variable (ΔE_0) for all fit paths in a given dataset. The amplitude reduction factors (S_0^2) were fixed to a value of 1.0, and the coordination numbers (CN) were varied systematically based on a structural model to achieve the best fit to the EXAFS data. The best choice of all available FEFF paths and the goodness of the overall fit were optimized based on a combination of weighted F-factor (F) as well as visual fit to the EXAFS data and their Fourier transform. On the basis of studies of complexes of known structures, the uncertainties in final distances are within 0.02 Å.[11] The EXAFS data were fit using DFT structures in figure S3.

NRVS spectroscopy. NRVS spectra were collected at the APS in Argonne, at beamline 3-ID-D. NRVS scans were acquired in 8–15 scans at 1 h per scan. Energy calibration was performed using an $[FeCl_4]^-$ standard.[12] NRVS cells (Delrin, covered with Kapton tape) were loaded under an inert N_2 atmosphere with zeolite powder suspended in perfluoro-2-methylpentane, and then frozen under liquid nitrogen. Samples were loaded from liquid nitrogen into a precooled cryostat, ensuring the cryostat temperature remained below 140 K. Samples were measured in a grazing angle of 4°. The cryostat temperature was held at 10–15 K, whereas the actual sample temperature (between 90–110 K) was determined using the detailed balance relationship between Stokes/anti-Stokes spectral intensity.[13] The phoenix 2.1.4 software package[14,15] was used to add the scans, subtract the resonant peak, correct for background counts, and convert the resulting spectra to a partial density of states.[16]

DFT calculations. Cluster models were generated from crystallographic coordinates of BEA polymorph A, as outlined in refs 1 and 17, but only including T-sites directly connected to the β-6MR ligand, and with capping hydrides at 1.42 Å instead of capping hydroxyls to reduce computation times (see Supplementary Tables 1–6 for coordinates). Spin-unrestricted DFT calculations were performed with Gaussian 09 (revision D.01)[18] using the B3LYP functional. The 6-311G* basis set was used for Fe, for atoms directly coordinated to Fe, and for C_6H_6. The 6-31G* basis set was used for all other atoms. For geometry optimizations, the six T-sites of the β-6MR ligand were allowed to relax, and all other atoms were frozen at their crystallographic positions. For the C_6H_6 reaction

coordinate, all transition states were verified to contain a single imaginary frequency corresponding to motion along the reaction coordinate. Intrinsic reaction coordinate calculations were performed to further verify that each transition state connects the appropriate reactants and products. Mössbauer quadrupole splittings were calculated using the B3LYP functional, with the TZVP basis set on Fe and coordinating O atoms, and 6-31G* on all other atoms. Mössbauer isomer shifts were calculated with the ORCA computational package (version 303)[19] using the B3LYP functional. The CP(PPP) basis set was used on Fe, with 6-311G* on coordinating O atoms and 6-31G* on all others. A calibration curve was generated by relating the DFT-calculated electron densities at the iron nucleus $|\psi_0|^2$ values to the experimental isomer shifts for a test set of 23 structurally defined Fe complexes.[1] The IS values of the cluster models were then estimated from the value of $|\psi_0|^2$ calculated for each cluster model. NRVS spectra were simulated using larger cluster models constructed according to procedures outlined in ref 17. NRVS spectra were generated from frequency calculations using the gennrvs script.

Quantitation of Fe(III) Poisoned Sites. In Fe-BEA, the intensity of the Fe(III)-phenolate charge transfer is double that of the 15,900 cm^{-1} $d_{z2} \rightarrow d_{x2-y2}$ ligand field transition of α-Fe(II). This intensity ratio can be used to estimate the ratio of phenolate poisoned sites. This requires reasonable estimates of molar extinction coefficients for the absorption features of interest. Studies of structurally defined model complexes define typical values of ε=3000-6000 $M^{-1}cm^{-1}$ for S=5/2 Fe(III)-phenolate charge

transfers[20–23] and ε=10-93 $M^{-1}cm^{-1}$ for S=2 square planar Fe(II) $d_{z2} \rightarrow d_{x2-y2}$ ligand field bands.[24–27] Assuming an ε=10 $M^{-1}cm^{-1}$ for the α-Fe(II) $d_{z2} \rightarrow d_{x2-y2}$ transition and an ε=6000 $M^{-1}cm^{-1}$ for the Fe(III)-phenolate charge transfer provides a conservative lower bound for site poisoning of 0.2%, while Mössbauer data set an upper limit of 5%.

Activation of α-O for aromatic hydroxylation. Past studies have identified two contributions to the activation of α-O for electrophilic chemistry.[1,17] First, there is an unusually large Fe(IV)/Fe(III) reduction enthalpy. This derives from the vacant *trans* axial position and S=2 electronic structure of α-O, both of which stabilize the redox-active α-d_{z2}-derived molecular orbital. In aromatic hydroxylation, this leads to a large enthalpic driving force for C-O bond formation (ΔH=-15.5 kcal/mol from figure 4, versus ca. +5 kcal/mol for other Fe(IV)=O intermediates). As shown in figure S10, the driving force is diminished by ~10 kcal/mol on the triplet surface. This leads to a small activation barrier for C-O bond formation of $\Delta E^{\ddagger}$=2.3 kcal/mol – significantly lower than those predicted for other Fe(IV)=O intermediates (ca. 15 kcal/mol).[28,29] For α-O, C-O bond formation is almost thermoneutral, and the small $\Delta E^{\ddagger}$ therefore reflects the high intrinsic reactivity of the Fe=O core of α-O. From experiment, this Fe=O core is unusually covalent, with the highest Fe(IV)=O stretching frequency yet defined (885 cm^{-1}).[17] This makes a second important contribution to lowering activating α-O for aromatic hydroxylation: DFT calculations show high Fe=O covalency results in an α-d_{z2}-derived reactive FMO with ~50% oxo 2p content[1,17] that is an efficient acceptor orbital for electrophilic attack on C_6H_6.[30]

Evaluation of reaction mechanisms. Starting from the σ-complex in figure 4, three potential reaction mechanisms to form Fe(II) products were evaluated. The associated intramolecular H/D KIEs were estimated by comparing the two possible σ-complexes formed from benzene-1,3,5-d_3. Values of α were estimated using the Eyring model ($\alpha=\exp(-\Delta\Delta H^{\ddagger}/RT)$). In these calculations, the effective temperature was adjusted to 800-2300 K to account for 2.5±1.5 kcal/mol of free energy released during C-O bond formation. For the NIH shift discussed in the main text, the H/D $\Delta\Delta H^{\ddagger}$=+0.23 kcal/mol combined with an effective temperature of 800-2300 K results in a predicted α=1.05-1.16. This assumes an equilibrium between free benzene and the σ-complex. However if σ-complex formation is irreversible and barrier-less, this would result in an intramolecular KIE of unity. There is an H/D $\Delta\Delta H^{\ddagger}$=+1.69 kcal/mol predicted for homolysis of the ipso C-H bond of the σ-complex to form the Fe(III)-phenolate poisoned site. This correlates to a predicted α=1.44-2.89 (again, assuming an effective temperature of 800-2300 K). A second potential reaction mechanism involves transferring the ipso proton to the oxygen, directly forming the phenol ligated active site (intermediate 5 in figure 4). The barrier for this reaction is much higher than for the NIH shift ($\Delta\Delta H^{\ddagger}$=14.4 kcal/mol). A third mechanism would involve transfer of the ipso proton to the lattice, directly forming intermediate 4. However attempts to locate the associated transition state instead yielded the NIH shift transition state.

SI References

(1) Snyder, B. E. R.; Vanelderen, P.; Bols, M. L.; Hallaert, S. D.; Böttger, L. H.; Ungur, L.; Pierloot, K.; Schoonheydt, R. A.; Sels, B. F.; Solomon, E. I. The Active Site of Low-Temperature Methane Hydroxylation in Iron-Containing Zeolites. *Nature* **2016**, *536*, 317–321.

(2) Gunnlaugsson, H. P. Spreadsheet Based Analysis of Mössbauer Spectra. *Hyperfine Interact.* **2016**, *237*, 79.

(3) Solomon, E. I.; Pavel, E. G.; Loeb, K. E.; Campochiaro, C. Magnetic Circular Dichroism Spectroscopy as a Probe of the Geometric and Electronic Structure of Non-Heme Ferrous Enzymes. *Coord. Chem. Rev.* **1995**, *144*, 369–460.

(4) Cramer, S. P.; Tench, O.; Yocum, M.; George, G. N. A 13-Element Ge Detector for Fluorescence EXAFS. *Nucl. Instruments Methods Phys. Res. Sect. A Accel. Spectrometers, Detect. Assoc. Equip.* **1988**, *266*, 586–591.

(5) Scott, R. A.; Hahn, J. E.; Doniach, S.; Freeman, H. C.; Hodgson, K. O. Polarized X-Ray Absorption Spectra of Oriented Plastocyanin Single Crystals. Investigation of Methionine-Copper Coordination. *J. Am. Chem. Soc.* **1982**, *104*, 5364–5369.

(6) Scott, R. A. [23] Measurement of Metal-Ligand Distances by EXAFS. *Methods Enzymol.* **1985**, *117*, 414–459.

(7) DeWitt, J. G.; Bentsen, J. G.; Rosenzweig, A. C.; Hedman, B.; Green, J.; Pilkington, S.; Papaefthymiou, G. C.; Dalton, H.; Hodgson, K. O.; Lippard, S. J. X-Ray Absorption, Mössbauer, and EPR Studies of the Dinuclear Iron Center in the Hydroxylase Component of Methane Monooxygenase. *J. Am. Chem. Soc.* **1991**,

113, 9219–9235.

(8) Cramer, S. P.; Hodgson, K. O. X-Ray Absorption Spectroscopy: A New Structural Method and Its Applications to Bioinorganic Chemistry. *Prog. Inorg. Chem.* **1979**, *25*, 1–39.

(9) Tenderholt, A.; Hedman, B.; Hodgson, K. O. PySpline: A Modern, Cross-Platform Program for the Processing of Raw Averaged XAS Edge and EXAFS Data. In *13th International Conference on X-ray Absorption Fine Structure - XAFS13*; Hedman, B., Pianetta, P., Eds.; American Institute of Physics Conference Proceedings: Melville, New York, 2007; Vol. 882, pp 105–107.

(10) George, G. N.; Pickering, I. EXAFSPAK & EDG_FIT. Stanford Synchrotron Radiation Laboratory, Stanford Linear Accelerator Center, Stanford University: Stanford, CA 2000.

(11) Cramer, S. P.; Hodgson, K. O.; Stiefel, E. I.; Newton, W. E. A Systematic X-Ray Absorption Study of Molybdenum Complexes. The Accuracy of Structural Information from Extended X-Ray Absorption Fine Structure. *J. Am. Chem. Soc.* **1978**, *100*, 2748–2761.

(12) Smith, M. C.; Xiao, Y.; Wang, H.; George, S. J.; Coucouvanis, D.; Koutmos, M.; Sturhahn, W.; Alp, E. E.; Zhao, J.; Cramer, S. P. Normal-Mode Analysis of FeCl4- and Fe2S2Cl42- via Vibrational Mössbauer, Resonance Raman, and FT-IR Spectroscopies. *Inorg. Chem.* **2005**, *44*, 5562–5570.

(13) Zhao, J. Y.; Sturhahn, W. High-Energy-Resolution X-Ray Monochromator Calibration Using the Detailed-Balance Principle. *J. Synchrotron Radiat.* **2012**, *19*,

602–608.

(14) Sturhahn, W. CONUSS and PHOENIX: Evaluation of Nuclear Resonant Scattering Data. *Hyperfine Interact.* **2000**, *125*, 149–172.

(15) Sturhahn, W. NRIXS Software. http://www.nrixs.com 2017.

(16) Sturhahn, W.; Toellner, T. S.; Alp, E. E.; Zhang, X.; Ando, M.; Yoda, Y.; Kikuta, S.; Seto, M.; Kimball, C. W.; Dabrowski, B. Phonon Density of States Measured by Inelastic Nuclear Resonant Scattering. *Phys. Rev. Lett.* **1995**, *74*, 3832.

(17) Snyder, B. E. R.; Böttger, L. H.; Bols, M. L.; Yan, J. J.; Rhoda, H. M.; Jacobs, A. B.; Hu, M. Y.; Zhao, J.; Alp, E. E.; Hedman, B.; et al. Structural Characterization of a Non-Heme Iron Active Site in Zeolites That Hydroxylates Methane. *Proc. Natl. Acad. Sci.* **2018**, *115*, 4565–4570.

(18) Frisch, M. J.; Trucks, G. W.; Schlegel, H. B.; Scuseria, G. E.; Robb, M. A.; Cheeseman, J. R.; Scalmani, G.; Barone, V.; Mennucci, B.; Petersson, G. A.; et al. Gaussian09. Gaussian, Inc.: Wallingford, CT 2009.

(19) Frank, N. The ORCA Program System. *Wiley Interdiscip. Rev. Comput. Mol. Sci.* **2011**, *2*, 73–78.

(20) Carrano, C. J.; Carrano, M. W.; Sharma, K.; Backes, G.; Sanders-Loehr, J. Resonance Raman Spectra of High- and Low-Spin Ferric Phenolates. Models for Dioxygenases and Nitrile Hydratase. *Inorg. Chem.* **1990**, *29*, 1865–1870.

(21) Bailey, N. A.; Cummins, D.; McKenzie, E. D.; Worthington, J. M. Iron(III) Compounds of Phenolic Ligands. The Crystal and Molecular Structure of iron(III) Compounds of the Sexadentate Ligand N,N′-Ethylene-Bis-(O-

Hydroxyphenylglycine). *Inorganica Chim. Acta* **1981**, *50*, 111–120.

(22) Davies, J. E.; Gatehouse, B. M. The Crystal and Molecular Structure of Chlorobis-({\it N}-{\it N}-propylsalicylaldiminato)iron(III). *Acta Crystallogr. Sect. B* **1972**, *28*, 3641–3645.

(23) Carrano, C. J.; Spartalian, K.; Rao, G. V. N. A.; Pecoraro, V. L.; Sundaralingam, M. The iron(III) Complex of N-[2-((O-Hydroxyphenyl)glycino)ethyl]salicylidenimine. A Model Complex for the iron(III) Environment in the Transferrins. *J. Am. Chem. Soc.* **1985**, *107*, 1651–1658.

(24) Burns, R. G.; Clark, M. G.; Stone, A. J. Vibronic Polarization in the Electronic Spectra of Gillespite, a Mineral Containing Iron (II) in Square-Planar Coordination. *Inorg. Chem.* **1966**, *5*, 1268–1272.

(25) Pinkert, D.; Demeshko, S.; Schax, F.; Braun, B.; Meyer, F.; Limberg, C. A Dinuclear Molecular Iron (II) Silicate with Two High-Spin Square-Planar FeO4 Units. *Angew. Chemie Int. Ed.* **2013**, *52*, 5155–5158.

(26) Pinkert, D.; Keck, M.; Tabrizi, S. G.; Herwig, C.; Beckmann, F.; Braun-Cula, B.; Kaupp, M.; Limberg, C. A High-Spin Square Planar Iron(ii)-Siloxide and Its Tetrahedral Allogon - Structural and Spectroscopic Models of Fe-Zeolite Sites. *Chem. Commun.* **2017**, *53*, 8081–8084.

(27) Cantalupo, S. A.; Fiedler, S. R.; Shores, M. P.; Rheingold, A. L.; Doerrer, L. H. High-Spin Square-Planar CoII and FeII Complexes and Reasons for Their Electronic Structure. *Angew. Chemie Int. Ed.* **2012**, *51*, 1000–1005.

(28) de Visser, S. P.; Oh, K.; Han, A.-R.; Nam, W. Combined Experimental and

Theoretical Study on Aromatic Hydroxylation by Mononuclear Nonheme Iron (IV)–Oxo Complexes. *Inorg. Chem.* **2007**, *46*, 4632–4641.

(29) Neidig, M. L.; Decker, A.; Choroba, O. W.; Huang, F.; Kavana, M.; Moran, G. R.; Spencer, J. B.; Solomon, E. I. Spectroscopic and Electronic Structure Studies of Aromatic Electrophilic Attack and Hydrogen-Atom Abstraction by Non-Heme Iron Enzymes. *Proc. Natl. Acad. Sci.* **2006**, *103*, 12966–12973.

(30) Snyder, B. E. R.; Bols, M. L.; Schoonheydt, R. A.; Sels, B. F.; Solomon, E. I. Iron and Copper Active Sites in Zeolites and Their Correlation to Metalloenzymes. *Chem. Rev.* **2018**, *118*, 2718–2768.

Supporting Figures

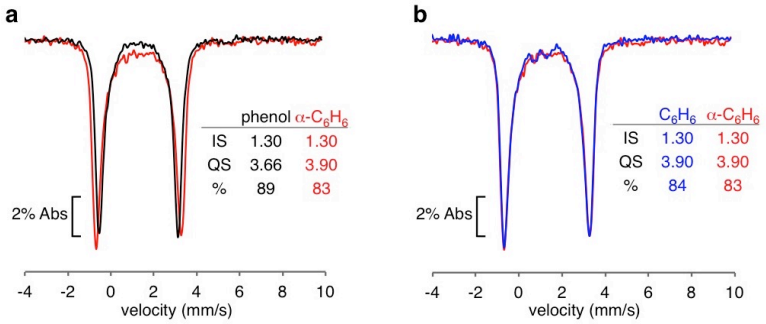

Figure S1. **a**, Comparison of 6K ^{57}Fe Mössbauer spectra and parameters of α-C_6H_6 (the single turnover product – red trace) and phenol-ligated α-Fe(II) (black trace). **b**, Comparison of data from α-C_6H_6 (red trace) with benzene-ligated α-Fe(II) (blue trace).

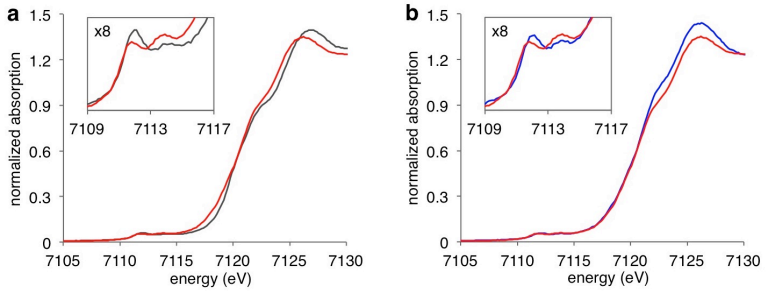

c EXAFS fits

scattering path	CN	r (Å)	σ^2 (Å^2)	χ^2
α-C_6H_6				
Fe-O	4	2.10	617	
Fe-Al	2	2.92	420	
Fe-Si	4	3.38	530	
Fe-Ob	2	3.41	673	
Fe-O	4	4.09	751	
Fe-O	4	4.70	839	
Fe-Si-O	4	3.57	261	
E_0 = -6.0169				0.29
α-Fe(II) + phenol				
Fe-O	5	2.09	683	
Fe-Al	2	2.90	444	
Fe-Si	4	3.35	839	
Fe-Ob	2	3.42	117	
Fe-O	4	4.06	866	
Fe-O	4	4.70	839	
Fe-Si-O	4	3.54	154	
E_0 = -6.4206				0.67
α-Fe(II) + benzene				
Fe-O	4	2.10	608	
Fe-Al	2	2.92	377	
Fe-Si	4	3.34	551	
Fe-O	4	4.00	425	
Fe-O	4	4.68	319	
E_0 = -7.3265				0.74

Figure S2. **a**, Comparison of Fe K-edge XANES of α-C_6H_6 (red trace) and phenol-ligated α-Fe(II) (black trace). The pre-edge region is shown in the inset. **b**, Comparison of data from α-C_6H_6 (red trace) and benzene-ligated α-Fe(II) (blue trace). **c**, Full EXAFS fits of α-C_6H_6 (top), phenol-ligated α-Fe(II) (middle), and benzene-ligated α-Fe(II) (bottom). CN = coordination number.

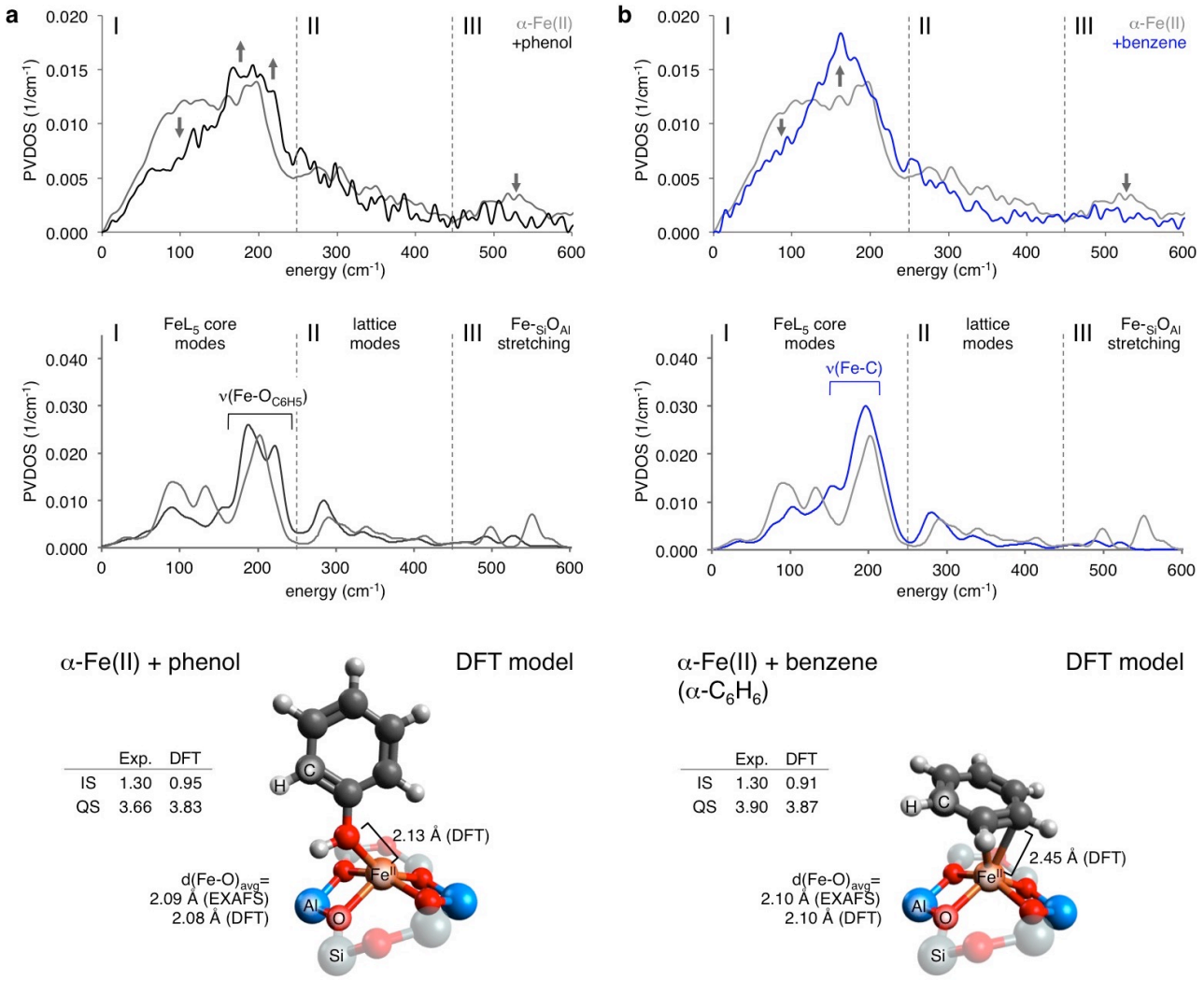

Figure S3. **a,** comparison of experimental (top) and simulated NRVS spectra (middle) from α-Fe(II) (gray trace) and phenol-ligated α-Fe(II) (black trace). Key spectral changes are indicated with arrows. From past studies, the NRVS intensity lost at ca. 100 cm^{-1} in α-Fe(II) corresponds to out-of-plane translation of the Fe center. In the presence of an axial ligand, OOP Fe motion is transferred into the new Fe-L stretching mode at higher frequency. This leads to additional intensity in the 175-250 cm^{-1} region in the experimental and simulated data associated with the Fe-O stretch of the phenol ligand. The DFT model of phenol-ligated α-Fe(II) used to simulate NRVS data is presented below (atoms have been omitted for clarity). Predicted bond lengths and MB parameters are compared to experimental data. **b,** comparison of experimental (top) and simulated NRVS spectra (middle) from α-Fe(II) (gray trace) and benzene-ligated α-Fe(II) (blue trace). Simulations indicate the additional intensity in the 125-200 cm^{-1} region of the benzene-ligated spectrum is related to the Fe-C stretching mode of the weakly bound π-η^2-C_6H_6 ligand. The DFT model of benzene-ligated α-Fe(II) used to simulate NRVS data is presented below, with predicted bond lengths and MB parameters are compared to experimental data.

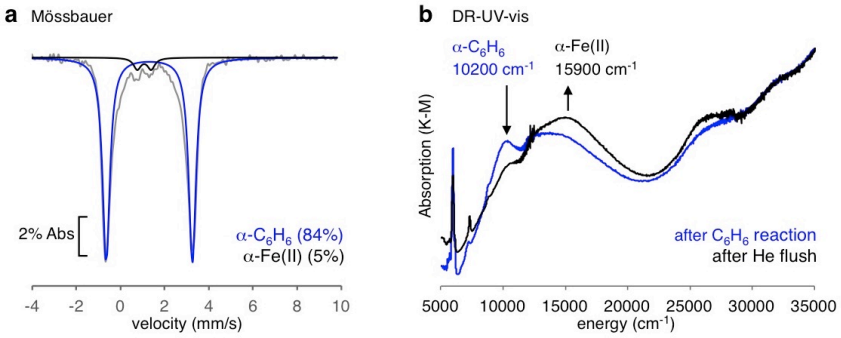

Figure S4. **a,** 6K Mössbauer spectrum of Fe(II)-BEA with C_6H_6 adsorbed (gray trace – reproduced from figure 1b), showing an equilibrium between α-C_6H_6 (blue component, 84%) and α-Fe(II) (black component) in the presence of excess benzene. **b,** 300K DR-UV-vis data from N_2O activated Fe-BEA after reacting with C_6H_6 at room temperature (blue trace), and subsequent flush with He. As benzene desorbs from α-C_6H_6, the band at 10,200 cm^{-1} decays, while the 15900 cm^{-1} band of α-Fe(II) grows in. The 10,200 cm^{-1} feature is therefore assigned as an S=2 Fe(II) ligand field band of α-C_6H_6. The 15,900 cm^{-1} band of pure α-Fe(II) is ca. 50% as intense as the 14,400 cm^{-1} band of the Fe(III)-phenolate impurity. Using the phenolate band as an internal standard leads to an estimate of 25-50% recovery of α-Fe(II) following the He flush.

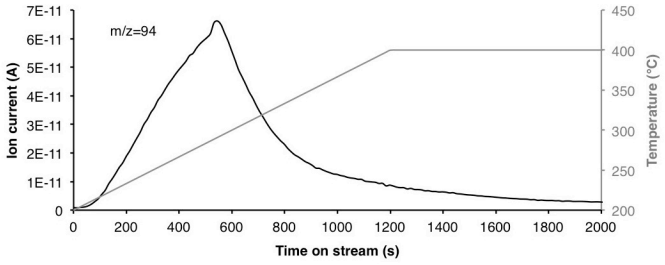

Figure S5. Temperature programmed desorption of phenol (m/z=94) from Fe-BEA, produced by the reaction of C_6H_6 with α-O at room temperature. The experiment was performed in a 20 ml/min (at STP) flow of He, using a heating ramp of 10 ºC/min from 200-400 ºC.

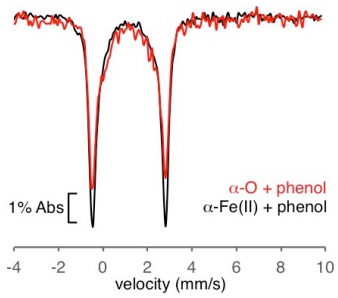

Figure S6. Comparison of 300K ^{57}Fe Mössbauer spectra from the room temperature reaction of phenol vapor with α-O (red trace) and phenol-ligated α-Fe(II) (black trace) in Fe-BEA.

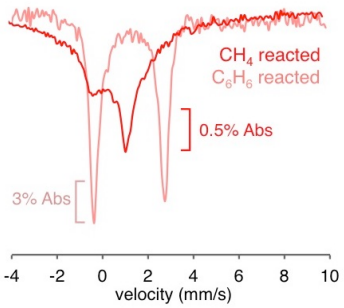

Figure S7. Comparison of 300K ^{57}Fe Mössbauer spectra from α-O (BEA) reacted at room temperature with CH_4 (red trace, 50% ^{57}Fe enrichment, reproduced from ref 9) and C_6H_6 (pink trace, 100% ^{57}Fe enrichment). While the C_6H_6 reacted results in clean regeneration of the Fe(II) active site, the CH_4 reaction results in significant heterogeneity (including some ferric iron).

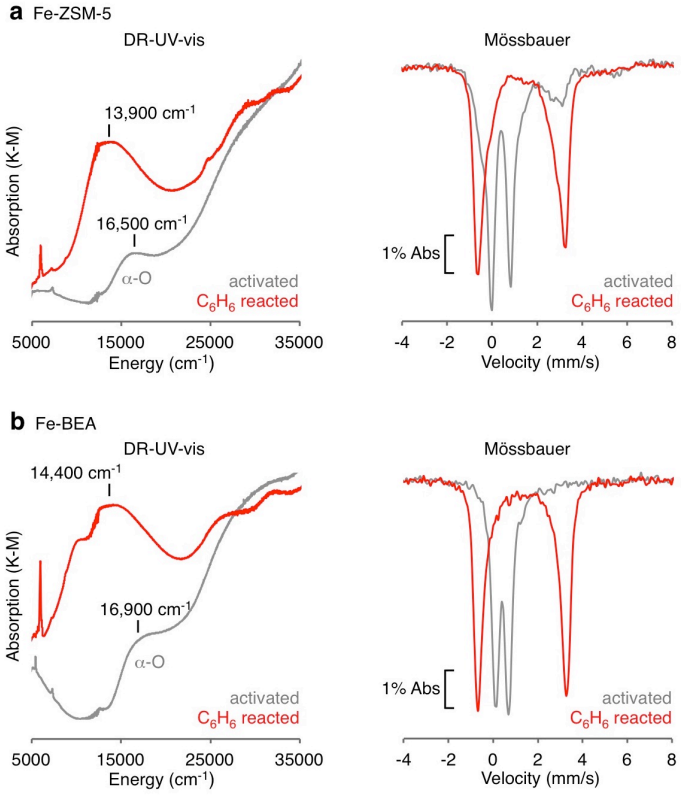

Figure S8. Comparison of spectroscopic data tracking the reaction of α-O (gray traces) with benzene (red traces) in Fe-ZSM-5 (**a**) and Fe-BEA (**b**). In DR-UV-vis spectroscopy (left), there is an absorption feature that appears at ca. 14,000 cm^{-1} in both Fe-BEA and Fe-ZSM-5 following reaction with C_6H_6. The 6K ^{57}Fe Mössbauer spectroscopy of the C_6H_6 reaction (right) is similar for Fe-BEA and Fe-ZSM-5, with reduction of α-O to form a new S=2 Fe(II) species with a large quadrupole splitting (α-C_6H_6).

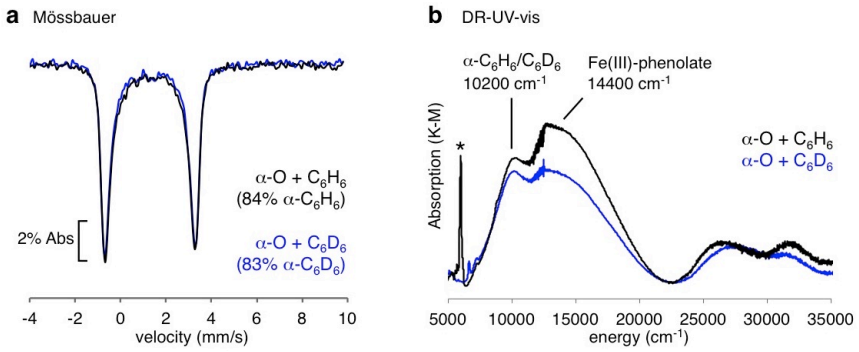

Figure S9. **a,** comparison of 6K ^{57}Fe Mössbauer spectra from α-O (BEA) reacted at room temperature with C_6H_6 (black trace) and C_6D_6 (blue trace), showing the same quantities of α-C_6H_6/C_6D_6 form. **b**, comparison of parallel DR-UV-vis data showing a 25-35% decrease in the 14,400 cm^{-1} ferric phenolate charge transfer band upon substrate deuteration. The 10,200 cm^{-1} ligand field band of α-C_6H_6/C_6D_6 remains constant, and serves as an internal standard for this comparison. The starred peak is a vibrational overtone of C_6H_6 that shifts below 5000 cm^{-1} for C_6D_6.

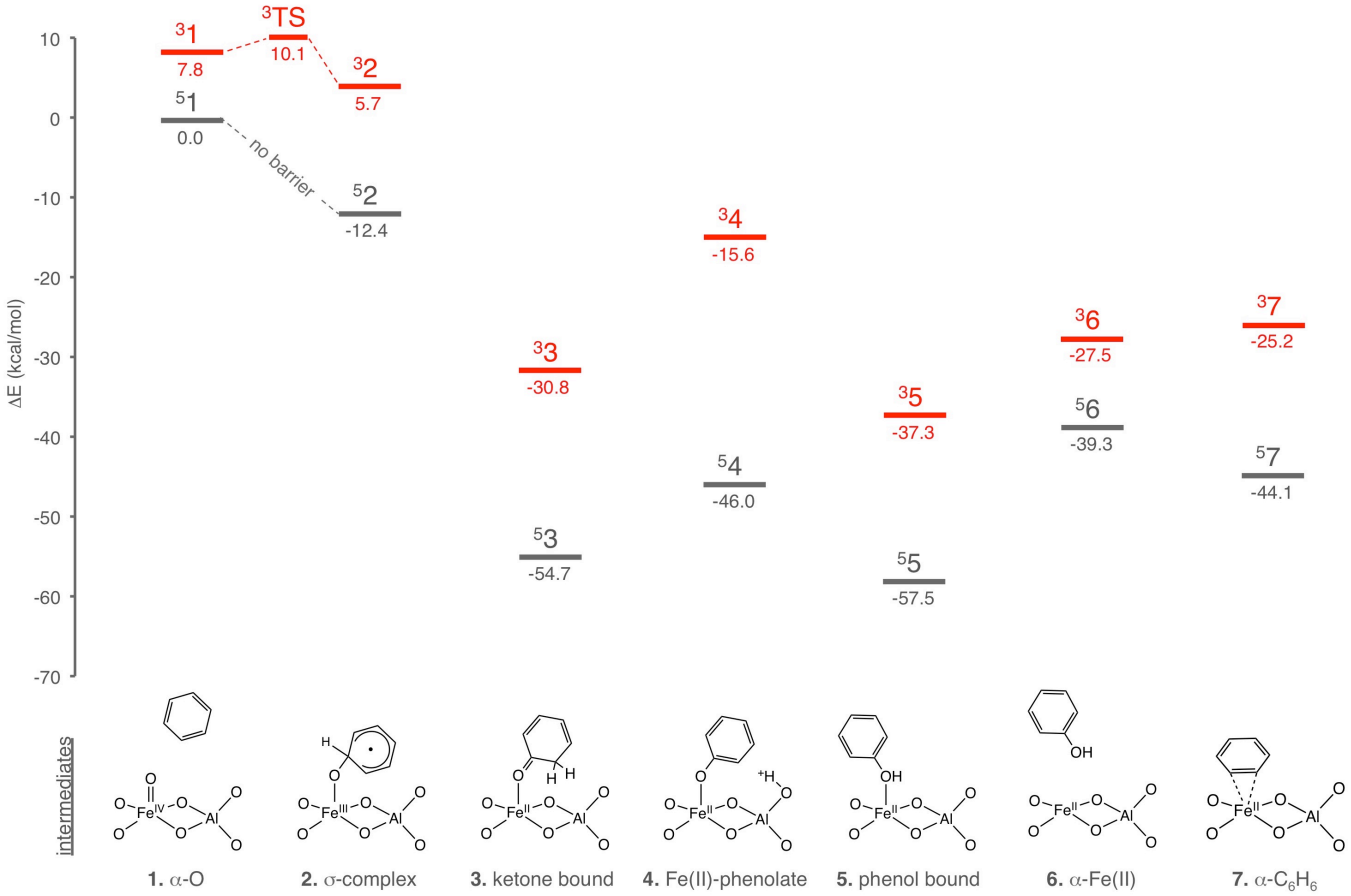

Figure S10. Intermediates in benzene hydroxylation by α-O, and their relative energies (ΔE) on the quintet (gray) and triplet surfaces (red). For this reaction coordinate, the triplet surface is well separated from the lower energy quintet surface, and it does not contribute to reactivity. There is a small 2.3 kcal/mol barrier for C-O bond formation on the triplet surface due to the loss of ~10 kcal/mol of driving force for this reaction (relative to the quintet surface).

Supplementary Tables

Table S1 – Coordinates of C_6H_6-ligated α-Fe(II) (DFT NRVS model)

element	constrained during optimization?	X	Y	Z
Fe	N	0.02976407	-0.83328513	-2.55127621
O	N	1.12515416	-1.92036418	-1.10626438
O	N	-1.09775000	0.90019107	-2.10948315
O	N	-1.73626074	-1.59177572	-1.72045657
O	N	1.75071755	0.33966302	-2.25752137
O	Y	2.71475794	-5.34071911	4.59728148
O	Y	2.77363525	-6.80535193	0.28574311
O	Y	1.78284797	-3.06103960	3.67563759
O	Y	-1.84372180	4.70759209	1.03080376
O	Y	4.36851088	-3.51173810	3.68473657
O	Y	5.86961330	0.99152132	4.17266020
O	Y	-6.08067231	3.23019283	1.63972262
O	Y	-5.95757500	1.75996687	3.81638330
O	Y	6.01763540	-1.49497490	3.33007697
O	Y	2.81232683	-4.82660859	2.02051334
O	Y	-2.83971040	5.10794899	-1.37009164
O	Y	3.59255598	1.40609396	-6.78601770
O	N	1.85936514	-4.44019732	-0.45227956
O	Y	-3.52032342	-5.18512650	-4.62609039
O	N	-1.85025424	3.31222908	-3.08356230
O	Y	4.39957402	-4.77826601	-0.07791726
O	Y	2.70469567	4.07847649	3.08081404
O	Y	-6.02183378	1.76556210	-2.67181836
O	Y	-2.79225362	-1.34310754	4.86033748
O	Y	6.03004169	-2.93570026	-0.98990540
O	Y	5.98218952	-1.53387373	-3.21088440
O	Y	-0.63986327	-2.03802053	3.52445458
O	Y	-5.94806023	-0.69363455	-3.59217902
O	Y	0.57584351	3.81348903	1.56487304
O	Y	4.82158362	0.18528338	-4.81582306
O	N	0.49267004	-2.98109228	1.32463353
O	Y	-4.77151190	-3.02755202	-3.81399938
O	N	-0.52103021	3.21557285	-0.77138345
O	Y	1.39567939	-0.77373735	2.42946002
O	Y	-1.44957340	2.13430395	1.42721465
O	N	2.64494975	1.61663016	-4.38689176
O	N	-0.62301904	-3.88040899	-0.92751843

O	N	-2.60690150	-3.94500749	-2.56788887
O	N	0.64135803	2.61042011	-3.09825644
O	Y	4.92571671	2.81411853	-5.00834963
O	Y	-4.88678205	-5.23822500	-2.37889625
O	Y	5.00180533	4.25415307	-1.06188504
O	Y	6.12573207	-0.31537261	-0.88882727
O	Y	-2.14940850	-0.07144170	2.65703026
O	Y	-6.13208220	-0.26083308	-1.00836888
O	Y	2.08831216	1.73020874	2.08562294
O	Y	4.75300349	1.80349167	-0.16176859
O	N	-2.80706122	0.33526797	0.16572002
O	Y	-4.78087976	-1.50199157	0.87215829
O	N	2.82787605	-0.11603839	0.37627066
O	Y	6.18487319	0.48746191	1.61252793
O	Y	-3.95591414	1.75732860	2.11311562
O	Y	-6.23231112	0.61187787	1.46815789
O	Y	3.89348390	-0.04615382	2.78499103
O	N	3.04435853	2.72730865	-1.98676978
O	N	-3.03988388	-3.28906960	-0.01014022
O	Y	2.98078470	3.63063324	0.50261724
O	N	-3.90048064	0.26287342	-2.45025441
O	Y	-3.02783079	-2.54669512	2.53229061
O	N	3.91154616	-1.60838811	-1.77890915
Si	Y	2.91986834	-4.18779827	3.49248818
Si	Y	-2.97224891	5.48863548	0.18678183
Si	Y	2.94902881	-5.21538753	0.46504276
Si	Y	-2.95138453	4.47636953	-2.84588257
Si	Y	0.76419793	-2.21639709	2.75907062
Si	Y	-0.81577086	3.48574220	0.82668706
Si	Y	4.01065973	1.51249540	-5.23460620
Si	N	0.73538276	-3.27408214	-0.25808906
Si	Y	-3.96267787	-4.33404446	-3.33241755
Si	N	-0.73202231	2.50432408	-2.22116291
Si	Y	-2.61544365	1.03728508	1.58640170
Si	Y	2.56448027	0.20202185	1.91034480
Si	Y	3.94736810	3.10022917	-0.67031952
Al	N	-2.53489038	0.00961722	-1.47258608
Si	Y	-3.97424121	-2.83830113	1.26319596
Al	N	2.55029763	-0.81659357	-1.13044603
Si	Y	5.50465949	-1.57666553	-1.67292620
Si	Y	-2.15379486	-1.50351885	3.39218244
Si	Y	-5.49317105	0.27275001	-2.38622691
Si	Y	2.08884936	3.31532113	1.80516335

Si	N	2.05400956	1.82939199	-2.88545231
Si	N	-2.03773255	-3.14768472	-1.26849029
Si	Y	5.49097111	-0.01542943	2.97427329
Si	Y	-5.55617701	1.83923852	2.25883715
O	Y	-5.02852955	-3.99939188	1.63343758
O	Y	-4.42693441	5.05917530	0.72718642
O	Y	-2.77779613	7.07593724	0.37251800
O	Y	-4.39590433	3.79269757	-3.03547918
O	Y	-2.76542959	5.63522064	-3.94743848
O	Y	4.97138748	3.46090863	4.26707078
O	Y	-5.07318367	-0.14527623	5.39799816
O	Y	3.49376636	5.43578337	5.18559316
O	Y	-3.61921628	-1.15545797	7.34548992
O	Y	4.76042701	5.69894681	2.89888677
Si	Y	3.98565317	4.66542580	3.85883324
Si	Y	-4.08751905	-1.34657486	5.81581778
O	Y	-4.85312042	-2.75403402	5.66479392
H	Y	3.39909062	-6.01932480	4.48728625
H	Y	3.45789246	-7.26581064	0.79625625
H	Y	5.05711096	-4.18611257	3.57547870
H	Y	6.83266562	1.01037074	4.28701442
H	Y	-7.04541446	3.27981107	1.72751855
H	Y	-6.92229105	1.80929182	3.90457000
H	Y	6.98071005	-1.47660148	3.44429508
H	Y	4.39142540	1.34384379	-7.33271918
H	Y	-4.31072931	-5.46990027	-5.11108196
H	Y	5.08687677	-5.23417295	0.43257565
H	Y	-6.98918281	1.75802648	-2.74289007
H	Y	6.99835890	-2.96784463	-1.03672114
H	Y	6.95072443	-1.56918764	-3.24994016
H	Y	-6.91571729	-0.69396236	-3.65899665
H	Y	5.61983026	0.10895317	-5.36080890
H	Y	-5.56228615	-3.30001685	-4.30534380
H	Y	5.72058625	2.75074606	-5.56064375
H	Y	-5.67297612	-5.52579044	-2.86887546
H	Y	4.52258477	5.03934037	-1.36957249
H	Y	7.09396224	-0.35094907	-0.93441769
H	Y	-7.09934688	-0.26486889	-1.08052473
H	Y	5.70598328	1.98125558	-0.19509848
H	Y	-5.73413228	-1.66837127	0.93935985
H	Y	7.14781369	0.50571744	1.72791357
H	Y	-7.19693785	0.66230105	1.55680639
H	Y	-4.54873284	-4.80841625	1.87027868

H	Y	-5.11047331	5.52679027	0.22220795
H	Y	-3.45702652	7.54650975	-0.13553540
H	Y	-5.08840034	4.46104946	-2.91480844
H	Y	-3.45487489	6.30723304	-3.82946034
H	Y	5.74190098	3.81831744	4.73555575
H	Y	-5.85232625	-0.15052353	5.97575393
H	Y	4.26333502	5.79102651	5.65726453
H	Y	-4.39745707	-1.15704404	7.92448339
H	Y	5.53342144	6.05512776	3.36419815
H	Y	-5.63469639	-2.76023054	6.23925340
H	N	0.01711038	-4.79705608	-4.53461130
H	N	-1.90965875	-3.45066681	-5.29077771
C	N	0.13107109	-3.72581639	-4.65013629
C	N	-0.96603976	-2.96136821	-5.05981658
C	N	1.35075093	-3.11678010	-4.35371079
C	N	-0.84002658	-1.57919666	-5.16767194
H	N	2.18871041	-3.70134886	-3.99483178
H	N	-1.69674690	-0.97324683	-5.43311245
C	N	1.49206718	-1.73137610	-4.48846937
C	N	0.38925705	-0.95344237	-4.89055516
H	N	0.51669879	0.10433845	-5.09743726
H	N	2.44902584	-1.26638359	-4.27278500

Table S2 – Coordinates of phenol-ligated α-Fe(II) (DFT NRVS model)

element	constrained during optimization?	X	Y	Z
Fe	N	0.17446788	-1.89066403	-1.53326630
O	N	-1.04439226	-0.41704573	-2.26376349
O	N	1.25153440	-2.05089318	0.21068544
O	N	1.85840615	-0.77663718	-1.99862375
O	N	-1.65491085	-2.30603552	-0.53933625
O	Y	-3.17620710	5.93942983	-3.69835874
O	Y	-2.77834085	2.36214057	-6.48810366
O	Y	-2.18317631	4.41015372	-1.80361268
O	Y	1.59884944	-0.29358977	4.83491166
O	Y	-4.75067242	4.32854865	-2.34228406
O	Y	-6.34830149	3.16983165	2.00233190
O	Y	5.76954567	1.15437058	3.82787527
O	Y	5.44354815	3.67202955	3.14253206

O	Y	-6.37957634	3.18084219	-0.62700806
O	Y	-3.01737033	3.33937364	-4.05618813
O	Y	2.82897047	-2.59020713	4.47594272
O	Y	-2.97348318	-7.05797855	-1.07212662
O	N	-1.82287377	0.97808151	-4.44979001
O	Y	3.96259112	-2.20752516	-6.27487560
O	N	2.03094664	-3.71764171	2.18537036
O	Y	-4.38338729	1.20471975	-4.76496940
O	Y	-3.12651869	1.42111130	4.70422724
O	Y	6.16742277	-2.42296850	1.03812136
O	Y	2.22643182	5.38098770	0.40980119
O	Y	-5.93490044	-0.40795264	-3.39483795
O	Y	-5.67841659	-2.95174682	-2.79189512
O	Y	0.22973838	4.15517908	-0.77800867
O	Y	6.21760756	-2.48715819	-1.58741862
O	Y	-0.85143147	0.27922365	4.05584606
O	Y	-4.38084407	-4.91832792	-1.63895249
O	N	-0.67063016	2.28438296	-2.42883934
O	Y	5.09837223	-2.03732089	-3.91666858
O	N	0.48548443	-1.62548028	2.79351783
O	Y	-1.69908883	2.52314605	-0.03174721
O	Y	1.19759004	0.88775024	2.51563467
O	N	-2.24593229	-4.80526695	-0.07770247
O	N	0.69463831	0.58450479	-3.96344707
O	N	2.82959889	-0.77861011	-4.45492112
O	N	-0.43776544	-3.69074445	1.38457158
O	Y	-4.49753045	-5.97221696	0.77666177
O	Y	5.09375703	0.04825018	-5.53217115
O	Y	-4.99225109	-2.74247370	3.41817566
O	Y	-6.07226210	-1.18236530	-0.89147707
O	Y	1.79545330	2.83273358	0.86435375
O	Y	6.13250422	-0.18350473	-0.32904916
O	Y	-2.38352575	1.31360821	2.19000460
O	Y	-4.80649439	-1.06843648	1.40798171
O	N	2.71473748	0.42919714	0.47100987
O	Y	4.61223973	1.86739256	-0.94961681
O	N	-2.89523002	0.23286739	-0.12614753
O	Y	-6.39532381	0.89977594	0.67855502
O	Y	3.62568370	1.88791198	2.49552793
O	Y	5.96969490	1.86705141	1.30596415
O	Y	-4.22878016	2.38825200	0.65913844
O	N	-2.95433818	-2.96289938	1.76929435
O	N	3.00043257	1.47917477	-3.02518372

O	Y	-3.13349312	-0.88072506	3.42942031
O	N	4.05565018	-1.92405475	-0.40971186
O	Y	2.71232163	3.60963807	-1.47430711
O	N	-3.77012719	-1.35461191	-2.32331223
Si	Y	-3.28186714	4.50333469	-2.97841506
Si	Y	2.79781859	-1.23954128	5.34834545
Si	Y	-2.99039466	1.99227171	-4.93597033
Si	Y	3.09792969	-3.75974656	3.40392703
Si	Y	-1.08692845	3.36498866	-1.25864745
Si	Y	0.61203174	-0.17866483	3.56851780
Si	Y	-3.54837373	-5.67300310	-0.48551979
Si	N	-0.73602134	0.88080916	-3.24817347
Si	Y	4.25981971	-1.23067458	-5.02976275
Si	N	0.85351508	-2.73190013	1.65893421
Si	Y	2.35483277	1.50510085	1.58455967
Si	Y	-2.82087414	1.60717429	0.66823171
Si	Y	-3.96911915	-1.89818136	2.50335879
Al	N	2.62256910	-1.02329807	-0.37600152
Si	Y	3.78632758	2.59972978	-2.12055889
Al	N	-2.50092836	-0.91404083	-1.29465458
Si	Y	-5.35941833	-1.44802814	-2.31008249
Si	Y	1.74269903	3.99482879	-0.24829966
Si	Y	5.63085826	-1.71293687	-0.30261207
Si	Y	-2.37482394	0.52936423	3.59572631
Si	N	-1.86568374	-3.39102976	0.66503522
Si	N	2.13160414	0.15615659	-3.32991188
Si	Y	-5.83748727	2.40893821	0.67810668
Si	Y	5.20177835	2.14467744	2.69230841
O	Y	4.81156754	3.42604068	-3.04931048
O	Y	4.19509507	-0.45650459	5.18395899
O	Y	2.56617112	-1.60421711	6.89922517
O	Y	4.56240912	-3.58034852	2.76130647
O	Y	3.01086560	-5.19300167	4.13139623
O	Y	-5.49444960	2.53025158	4.40555435
O	Y	4.42608965	5.70308646	1.81844805
O	Y	-4.14207296	2.88114797	6.63605532
O	Y	2.79394161	7.73162315	1.43328327
O	Y	-5.17263994	0.52848171	6.08323433
Si	Y	-4.48702584	1.84168079	5.45444047
Si	Y	3.41772129	6.39961390	0.77572474
O	Y	4.21178132	6.79045490	-0.56837711
H	Y	-3.83749117	5.99588081	-4.40577019
H	Y	-3.50531680	2.93024616	-6.78744235

H	Y	-5.41633055	4.38391128	-3.04565274
H	Y	-7.31814902	3.18242091	2.01417493
H	Y	6.71967623	1.30947377	3.94659218
H	Y	6.39361636	3.82759397	3.26109803
H	Y	-7.34942642	3.19345778	-0.61565989
H	Y	-3.71171996	-7.62502098	-1.34472848
H	Y	4.80152977	-2.49686775	-6.66643348
H	Y	-5.11345655	1.77101679	-5.06015328
H	Y	7.13703404	-2.39807657	1.05129779
H	Y	-6.89297802	-0.53061347	-3.48387465
H	Y	-6.63745584	-3.06607063	-2.88143245
H	Y	7.18698535	-2.46070030	-1.56609224
H	Y	-5.11951932	-5.47859799	-1.92402267
H	Y	5.93815260	-2.33697525	-4.29849699
H	Y	-5.23127411	-6.54375342	0.50133131
H	Y	5.92922046	-0.24544407	-5.92788022
H	Y	-4.49379162	-3.24534490	4.08116579
H	Y	-7.03032232	-1.30278780	-0.98333319
H	Y	7.10211686	-0.16092155	-0.31306262
H	Y	-5.75323373	-1.24596168	1.52226195
H	Y	5.55567594	2.07301939	-1.04212928
H	Y	-7.36515780	0.91354008	0.69017802
H	Y	6.91961410	2.02268103	1.42571368
H	Y	4.32000643	3.87029400	-3.75775110
H	Y	4.92071716	-1.02181126	5.49182393
H	Y	3.28779237	-2.17378699	7.20869591
H	Y	5.23085993	-3.62265850	3.46288589
H	Y	3.67650805	-5.23929849	4.83543647
H	Y	-6.31291662	2.78226691	4.86108838
H	Y	5.14242024	6.31968474	2.03655484
H	Y	-4.95989796	3.13695692	7.09062382
H	Y	3.50920473	8.34809914	1.65521040
H	Y	-5.99323710	0.77768853	6.53646406
H	Y	4.93087935	7.40449038	-0.35213098
O	N	-0.00040377	-3.91367959	-2.10178957
C	N	0.98776762	-4.84609470	-2.44176540
C	N	2.23118851	-4.36045103	-2.82149536
C	N	0.71619285	-6.20781980	-2.38567117
C	N	3.23323820	-5.26784407	-3.14962011
C	N	1.72939421	-7.10285734	-2.72413742
C	N	2.98674763	-6.63875767	-3.10574227
H	N	4.20708873	-4.87862823	-3.42334139
H	N	2.43093878	-3.29641458	-2.85499698

H	N	-0.80651903	-4.34542747	-1.77568704
H	N	-0.26006814	-6.56461041	-2.06946969
H	N	1.52981269	-8.16843383	-2.67884169
H	N	3.77264790	-7.34298622	-3.35773751

Table S3 – Coordinates of α-O (DFT model)

element	constrained during optimization?	X	Y	Z
Fe	N	-0.00006283	-0.00007343	-1.31138065
O	N	0.63336999	-1.70659091	-0.42556902
O	N	-0.63346383	1.70660593	-0.42594743
O	N	-1.87170493	-0.48518852	-0.87321511
O	N	1.87167244	0.48513937	-0.87315073
H	Y	0.94355851	-6.91769319	-0.68460900
H	Y	0.54696667	-4.28483304	3.58085100
H	Y	-0.54694309	4.28542742	3.58037449
H	Y	1.30888285	-5.80900975	1.32275064
H	Y	-1.30876779	5.80934075	1.32207373
H	Y	4.40308929	2.31090160	-4.67632700
O	N	0.69752526	-4.39221443	-0.71098174
H	Y	-4.40231907	-2.31037048	-4.67632196
O	N	-0.69748543	4.39230456	-0.71151988
H	Y	2.81517898	-5.57931619	-0.42951796
H	Y	-5.10757563	3.85504812	-0.78957785
H	Y	5.10779116	-3.85491185	-0.78892871
H	Y	5.54491729	-2.11103979	-2.25011002
H	Y	-1.26439671	-2.83935040	3.75921702
H	Y	-5.54465899	2.11097718	-2.25055763
H	Y	1.26439330	2.83998040	3.75893730
H	Y	5.02585157	0.49727834	-3.38176291
O	N	-0.41947213	-3.33468351	1.46556856
H	Y	-5.02572098	-0.49748947	-3.38195822
O	N	0.41931338	3.33502292	1.46512464
O	Y	0.95037001	-1.86687530	3.20213120
O	Y	-0.95025879	1.86731878	3.20172419
O	N	3.25330617	2.07127157	-2.54167365
O	N	-1.55309004	-3.11421943	-0.91641735
O	N	-3.25301336	-2.07214834	-2.54149609
O	N	1.55284810	3.11394344	-0.91725467
H	Y	5.73406005	2.63870795	-2.80278177

H	Y	-5.73386330	-2.63874195	-2.80269722
H	Y	5.84776633	2.70698483	1.47002861
H	Y	5.78369667	-1.79851587	0.03207344
H	Y	-2.30481986	-0.15876254	3.59164902
H	Y	-5.78354336	1.79873017	0.03167651
H	Y	2.30480392	0.15936776	3.59172572
H	Y	5.01176311	0.55170529	1.53484934
O	N	-2.76376123	0.96224573	1.45705853
H	Y	-5.01166752	-0.55132973	1.53472523
O	N	2.76379009	-0.96201547	1.45706691
H	Y	-3.37965691	1.89285767	3.66393380
H	Y	3.37967162	-1.89225460	3.66428510
O	N	3.83238456	2.11821432	0.05414741
O	N	-3.83290418	-2.11748820	0.05390475
H	Y	3.88031624	2.26541644	2.61657103
O	N	-3.44784084	2.01833124	-1.09033355
H	Y	-3.88023617	-2.26492815	2.61662869
O	N	3.44782763	-2.01840663	-1.09010103
Si	Y	1.44501418	-5.73048260	-0.08846717
Si	Y	-1.44496081	5.73066691	-0.08917568
Si	Y	-0.05928853	-3.11143929	3.05926650
Si	Y	0.05917730	3.11201531	3.05893203
Si	Y	4.67264204	1.87156608	-3.35310481
Si	N	-0.14182858	-3.15241323	-0.12211135
Si	Y	-4.67240602	-1.87258915	-3.35275611
Si	N	0.14179404	3.15248104	-0.12257652
Si	Y	-2.37060786	1.13587498	3.01210857
Si	Y	2.37063171	-1.13519506	3.01212683
Si	Y	4.66130685	1.92673336	1.48007791
Al	N	-2.33786355	1.13612308	-0.17744735
Si	Y	-4.66136280	-1.92636206	1.48015108
Al	N	2.33775480	-1.13609802	-0.17740222
Si	Y	5.02193671	-2.44968983	-0.97404320
Si	Y	-5.02197847	2.44966830	-0.97451467
Si	N	2.67275471	1.94767999	-1.05234578
Si	N	-2.67273402	-1.94782690	-1.05213307
H	Y	-5.84769303	-2.70662629	1.47011429
H	Y	-2.81504149	5.57946833	-0.43022555
H	Y	-0.94337355	6.91780733	-0.68540161
O	N	0.00050597	-0.00217628	-2.90191967

Table S4 – Coordinates of α-O/C_6H_6 σ-complex (DFT model)

element	constrained during optimization?	X	Y	Z
Fe	N	0.10466047	-0.16944672	-0.95395427
O	N	-0.95368300	1.55320027	-0.63989948
O	N	0.79129818	-1.41626827	0.51633952
O	N	1.76919214	0.81687949	-0.30309296
O	N	-1.77597705	-0.88171378	-0.57414609
H	Y	-2.00390481	6.37024599	-2.38287807
H	Y	-2.05776014	5.04080138	2.46614220
H	Y	0.30569274	-2.85055567	5.07125038
H	Y	-2.58372717	5.75748297	-0.21944786
H	Y	1.71941122	-4.71341378	3.47945586
H	Y	-3.16585326	-4.06768413	-4.04146284
O	N	-1.37565933	4.02322932	-1.65129389
H	Y	4.65981138	2.06701753	-4.06114773
O	N	1.30734223	-4.01506810	1.05848295
H	Y	-3.66333346	4.79388290	-2.03549208
H	Y	5.51681639	-2.63969869	1.48225039
H	Y	-5.55096806	2.61195816	-2.22205965
H	Y	-5.42184055	0.50330529	-3.17294117
H	Y	-0.11842296	4.08072489	3.31435080
H	Y	5.96204559	-1.27262635	-0.33438621
H	Y	-1.70379352	-1.79991046	4.56109123
H	Y	-4.29993848	-2.14841415	-3.42433524
O	N	-0.57008237	3.78432611	0.87310767
H	Y	5.28499569	0.80476039	-2.22636240
O	N	-0.34902790	-2.66987013	2.64773400
O	Y	-2.00614723	2.57570671	2.73758157
O	Y	0.40294473	-0.57766787	4.08254784
O	N	-2.50202395	-3.07962971	-1.92099857
O	N	1.04224572	3.21777677	-1.14942553
O	N	3.16453821	2.17235483	-2.14723238
O	N	-1.02722371	-3.30976104	0.16754365
H	Y	-4.77386434	-4.16953136	-2.36958761
H	Y	5.53124790	3.11983209	-2.18406717
H	Y	-5.71356137	-3.17238675	1.67974090
H	Y	-6.05423959	0.73907671	-0.95765000
H	Y	1.33009185	1.70974435	4.07355331
H	Y	5.69725858	-0.35002213	1.77315136
H	Y	-3.08649391	0.48610113	3.48479973
H	Y	-5.24442125	-0.94902910	1.24967448

O	N	2.36246892	0.18307152	2.44161578
H	Y	4.29662596	2.10089936	2.41262935
O	N	-3.28308700	0.92962343	1.07081844
H	Y	2.66909499	0.00176744	4.88560740
H	Y	-4.45399806	2.23086523	2.80993537
O	N	-3.59270242	-2.61344048	0.46409695
O	N	3.22480239	3.00522826	0.37826021
H	Y	-4.10043203	-2.06973212	2.92968041
O	N	3.68891385	-1.31151142	0.43401130
H	Y	2.72732205	3.77067391	2.78171535
O	N	-3.60617849	1.12612042	-1.73790941
Si	Y	-2.42618619	5.29765604	-1.55365327
Si	Y	2.11668734	-4.96989597	2.14050244
Si	Y	-1.18955258	3.91932265	2.39617709
Si	Y	-0.35746873	-1.99380079	4.15334662
Si	Y	-3.75420976	-3.37152765	-2.95257577
Si	N	-0.48989952	3.15340194	-0.62195009
Si	Y	4.72782743	2.04265007	-2.64297709
Si	N	0.19718390	-2.84694912	1.12780322
Si	Y	1.70464191	0.35062749	3.90351698
Si	Y	-3.23322561	1.55105545	2.55703075
Si	Y	-4.68507136	-2.19395730	1.64159225
Al	N	2.29459630	-0.45781977	0.86774799
Si	Y	3.75880147	3.31804589	1.91706100
Al	N	-2.56673776	0.74127031	-0.45958898
Si	Y	-5.21773825	1.25231870	-1.98393873
Si	Y	5.25629668	-1.37397798	0.89364066
Si	N	-2.26973275	-2.46111305	-0.44802428
Si	N	2.33473164	2.30672440	-0.77345024
H	Y	4.79120201	4.29141157	1.85995275
H	Y	3.48789307	-4.63918802	1.97641481
H	Y	1.92875719	-6.34505863	1.84053775
O	N	0.41888827	-0.61123097	-2.61516345
C	N	0.70953940	-1.28631384	-3.87245147
C	N	0.79822921	-2.76016021	-3.63477097
C	N	1.95275822	-0.69352051	-4.45415226
C	N	1.95056051	-3.45700400	-3.85308553
C	N	3.07876609	-1.43631235	-4.65842035
C	N	3.10630273	-2.81968242	-4.36298706
H	N	1.98362126	-4.51965723	-3.63304030
H	N	-0.08664646	-3.24406090	-3.23544901
H	N	-0.15951037	-1.05085854	-4.50366230
H	N	1.93513444	0.37051492	-4.66252725

H	N	3.97062210	-0.95996723	-5.05427024
H	N	4.01485868	-3.38952691	-4.52046357

Table S5 – Coordinates of NIH shift transition state (DFT model)

element	constrained during optimization?	X	Y	Z
Fe	N	0.15558268	-0.21104551	-0.95904982
O	N	0.96002756	-1.17581214	0.70155131
O	N	-1.19254106	1.35791526	-0.83824165
O	N	-1.63935520	-1.16993438	-0.57176285
O	N	1.62966212	1.10972249	-0.33542589
H	Y	2.78420336	-5.71389935	2.49447395
H	Y	0.48403706	-2.24566942	5.31651867
H	Y	-2.97066403	4.88923144	1.88078215
H	Y	2.24527520	-3.99415452	3.95876339
H	Y	-3.47885357	5.26268441	-0.87691996
H	Y	4.42455978	2.45192018	-4.11461376
O	N	1.83617058	-3.60806897	1.46585707
H	Y	-2.32950480	-4.83610255	-3.73601227
O	N	-1.93855782	3.63454950	-2.09295300
H	Y	4.04721768	-3.77384092	2.51081386
H	Y	-5.81823898	1.50993216	-2.65274299
H	Y	5.75637747	-1.52720513	1.88617318
H	Y	6.06381156	-0.27848337	-0.04085677
H	Y	-1.64025940	-1.58388703	4.64447414
H	Y	-5.31491188	-0.62845154	-3.38844677
H	Y	-0.94540641	4.33613102	2.87806542
H	Y	5.15572214	1.48041667	-2.14682987
O	N	-0.08209988	-2.41922611	2.88212842
H	Y	-3.77893213	-3.07638149	-3.34470016
O	N	-1.22775968	3.74896605	0.46748491
O	Y	0.26739861	-0.08707221	4.11378434
O	Y	-2.54390452	2.50006605	2.39340210
O	N	2.84623672	2.47268186	-2.27103330
O	N	-0.52150395	-3.35205573	0.43255243
O	N	-1.93165760	-3.58961143	-1.68832026
O	N	0.54610391	3.26600981	-1.43612549
H	Y	5.03198500	3.79892219	-2.32356356
H	Y	-3.97658269	-5.04221850	-2.11246554
H	Y	3.93137924	5.20133988	1.56182905
H	Y	5.56032545	0.77848686	1.95723004

H	Y	-3.31482095	0.34099914	3.30776597
H	Y	-6.07778401	-0.29579719	-1.22733807
H	Y	0.82203943	2.30931112	3.90968670
H	Y	3.76314921	3.01971532	2.31055006
O	N	-3.46755161	0.52397910	0.85760761
H	Y	-5.11459265	-1.62186654	1.15835378
O	N	2.18394967	0.82848853	2.48156842
H	Y	-4.90756264	1.77322926	2.42377507
H	Y	2.37461741	0.92116883	4.92569822
O	N	2.67492363	3.56681295	0.15353434
O	N	-3.17802875	-3.07353505	0.60544061
H	Y	1.93512053	4.44140569	2.46617072
O	N	-3.69223005	0.42333384	-1.96360169
H	Y	-3.88680931	-2.38482737	2.97426246
O	N	3.79347889	-0.61169264	0.63596127
Si	Y	2.73914705	-4.30480198	2.66417737
Si	Y	-3.18964441	4.71399992	-2.15430580
Si	Y	-0.26289530	-1.59474239	4.29927686
Si	Y	-1.93435475	3.92074514	1.94753998
Si	Y	4.43025720	2.56886765	-2.69942445
Si	N	0.55577451	-2.61916350	1.40136156
Si	Y	-3.06962694	-4.14710581	-2.73905194
Si	N	-0.98382825	2.99949795	-0.95609924
Si	Y	-3.58461576	1.27884023	2.27623119
Si	Y	1.41345804	1.01856397	3.88498978
Si	Y	3.06365365	4.08367628	1.68204968
Al	N	-2.65796225	0.31410757	-0.62671923
Si	Y	-4.38474502	-2.71914474	1.68711861
Al	N	2.26002533	0.04656085	0.97312067
Si	Y	5.32710513	-0.37933775	1.16889454
Si	Y	-5.28626507	0.24940378	-2.27267337
Si	N	1.94733800	2.61574946	-0.93313851
Si	N	-1.86586441	-2.78085795	-0.29293919
H	Y	-5.24689512	-3.84291112	1.78911555
H	Y	-4.30849237	3.97538058	-2.62240605
H	Y	-2.90390169	5.76009801	-3.07103851
O	N	0.85235731	-0.99430555	-2.44855597
C	N	2.05343182	-1.65964461	-2.71407830
C	N	2.77913243	-1.11184250	-3.89357800
C	N	1.93576040	-3.14644657	-2.70535657
C	N	3.44301231	-1.92251838	-4.76948919
C	N	2.61741718	-3.92344356	-3.59926356
C	N	3.38147075	-3.32596621	-4.62438653

H	N	3.99353158	-1.49593457	-5.60135319
H	N	2.77398126	-0.03269743	-3.99796921
H	N	2.76472990	-1.46344042	-1.86597482
H	N	1.31102480	-3.58127368	-1.93274846
H	N	2.54588852	-5.00469551	-3.54814255
H	N	3.90245492	-3.95732314	-5.33631149

Table S6 – Coordinates of 2,4-cyclohexadienone-ligated α-Fe(II) (DFT model)

element	constrained during optimization?	X	Y	Z
Fe	N	0.15298380	-0.15803609	-1.00517723
O	N	1.15110766	-0.97741020	0.66985677
O	N	-1.47204755	1.15155076	-0.82185618
O	N	-1.45609901	-1.44321635	-0.62890187
O	N	1.40150352	1.40787049	-0.38293585
H	Y	3.76884118	-5.12755760	2.37402279
H	Y	0.92743853	-2.14742139	5.25994370
H	Y	-3.79976879	4.27717477	1.93968310
H	Y	2.95272188	-3.54251911	3.86187753
H	Y	-4.40781304	4.57293826	-0.80721529
H	Y	3.82176005	3.24630599	-4.17784917
O	N	2.44554623	-3.22461643	1.37252993
H	Y	-1.51205154	-5.13622649	-3.77834211
O	N	-2.61686984	3.26229992	-2.06046371
H	Y	4.66424149	-2.99278957	2.39198273
H	Y	-6.06389221	0.47440018	-2.58732996
H	Y	5.93405370	-0.47197985	1.76598683
H	Y	5.98410281	0.82513951	-0.15293022
H	Y	-1.29082812	-1.87218041	4.62294236
H	Y	-5.19694709	-1.53399716	-3.35023847
H	Y	-1.69351923	4.08882531	2.90425540
H	Y	4.74439291	2.40768114	-2.22950426
O	N	0.37278948	-2.41624695	2.84199777
H	Y	-3.24707013	-3.66741887	-3.35067681
O	N	-1.90541728	3.49376201	0.49260766
O	Y	0.30989261	-0.05414526	4.08101366
O	Y	-2.94457052	1.99956153	2.42355085
O	N	2.28895764	2.99211912	-2.31582922
O	N	0.06361427	-3.37149595	0.37943945
O	N	-1.30492421	-3.86520354	-1.72439245
O	N	-0.10070558	3.33480795	-1.43389633

H	Y	4.20496307	4.66770010	-2.38228940
H	Y	-3.07114000	-5.64548113	-2.13482266
H	Y	2.92934151	5.82290314	1.53085252
H	Y	5.32948727	1.76073567	1.86180888
H	Y	-3.30274447	-0.26905897	3.32744010
H	Y	-5.97462165	-1.35859501	-1.17596157
H	Y	0.42345327	2.40420697	3.89248344
H	Y	3.16560872	3.64122096	2.26079145
O	N	-3.51317141	-0.10886309	0.88663525
H	Y	-4.75400627	-2.50741512	1.18370653
O	N	2.01935604	1.20068343	2.43746168
H	Y	-5.13920184	0.86086094	2.47876204
H	Y	2.21448325	1.30953700	4.87412803
O	N	1.96491553	4.01258702	0.12218666
O	N	-2.59577485	-3.59177644	0.59252822
H	Y	1.11513575	4.71130971	2.45464914
O	N	-3.77030270	-0.21351936	-1.93574482
H	Y	-3.38243791	-3.05084292	2.97551342
O	N	3.82323104	0.06641615	0.55216688
Si	Y	3.47479935	-3.75055495	2.55783749
Si	Y	-4.04419771	4.09393767	-2.09358752
Si	Y	0.06090608	-1.63369051	4.25914555
Si	Y	-2.60594044	3.50955449	1.98318283
Si	Y	3.82760566	3.35242465	-2.76180728
Si	N	1.00551479	-2.46930771	1.34753291
Si	Y	-2.34855929	-4.59799097	-2.76493967
Si	N	-1.55195135	2.79658936	-0.93613590
Si	Y	-3.75147924	0.61251253	2.30868206
Si	Y	1.23595158	1.24049250	3.84743633
Si	Y	2.27761674	4.56705732	1.65200827
Al	N	-2.70355681	-0.14864976	-0.61691270
Si	Y	-3.83168396	-3.45989009	1.69203932
Al	N	2.19600973	0.46437787	0.91259980
Si	Y	5.29553933	0.58543582	1.06560524
Si	Y	-5.30922439	-0.67308126	-2.22657549
Si	N	1.40506688	2.94903858	-0.96179539
Si	N	-1.37565549	-3.05552786	-0.32502246
H	Y	-4.47710411	-4.72061284	1.79484023
H	Y	-5.01961995	3.17014726	-2.55365254
H	Y	-3.96409509	5.18072379	-3.00399869
O	N	1.10268143	-0.80306591	-2.63847290
C	N	2.14201815	-1.39683487	-3.01029041
C	N	2.46973109	-1.47618431	-4.40570271

C	N	3.06640764	-2.04174304	-2.01524856
C	N	3.59050745	-2.13448743	-4.81088600
C	N	4.25414855	-2.74199661	-2.57237311
C	N	4.50011909	-2.77925991	-3.89471780
H	N	3.81508094	-2.18117364	-5.87266173
H	N	1.79622777	-1.00019570	-5.10844717
H	N	3.39964763	-1.28344502	-1.28406016
H	N	2.48362668	-2.73537502	-1.39334289
H	N	4.92261824	-3.21813356	-1.86269162
H	N	5.37255648	-3.28666668	-4.29000794